Semiconductors, Tunneling, and Micromagnetics

Gang Xiao and Philip L. Trouilloud, Chairmen

Very large magnetoresistance in electrodeposited single-crystal Bi thin films (invited)

C. L. Chien,[a] F. Y. Yang, Kai Liu, and D. H. Reich
Department of Physics and Astronomy, The Johns Hopkins University, Baltimore, Maryland 21218

P. C. Searson
Department of Materials Science and Engineering, The Johns Hopkins University, Baltimore, Maryland 21218

Single-crystal bismuth thin films, fabricated by electrodeposition and suitable annealing, exhibit very large magnetoresistance of 400 000% at 5 K and 300% at 300 K, as well as pronounced Shubnikov–de Haas oscillations. A hybrid structure demonstrates the potential for field sensing with sensitivities of 35%/Oe at 5 K and 0.2%/Oe at 300 K. © *2000 American Institute of Physics.* [S0021-8979(00)25508-4]

INTRODUCTION

Magnetoresistance (MR) effects in metals have received a great deal of attention in recent years because of their intricate physics and important applications. The first MR effect of importance is the anisotropic MR (AMR) effect in ferromagnetic metals and alloys.[1] The angular dependence of AMR is typically $\cos^2\theta$, where θ is the angle between the current **j** and the magnetization **M** of the ferromagnetic (FM) material. Both positive and negative AMR can be observed when **H** is applied parallel and perpendicular to the current. Even though the magnitude is relatively small (2%), the AMR effect in permalloy has already been extensively used in MR read heads and sensors for low magnetic fields. The discovery in 1988 of giant MR (GMR) in antiferromagnetically coupled magnetic multilayers (e.g., Co/Cu),[2,3] and subsequently in other geometries such as granular systems (e.g., Co particles in a Cu matrix),[4,5] has attracted worldwide attention. The term GMR now refers to MR effects due to spin-dependent scattering, which can be ''giant'' (as much as 150% in ideal cases)[6] or small (of order 10% in most cases). In the multilayer geometry, GMR varies as $\cos\theta$, where θ is the angle between the magnetizations of the two FM layers.[7] The original GMR effect in magnetic multilayers requires the application of a large magnetic field, and is thus technologically unattractive. Field sensors using the GMR effect became a reality with the development of spin-valve GMR structures with the structure AF/FM/Cu/FM, in which the bottom (pinned) FM layer is exchange biased by the antiferromagnetic layer.[7] Because the Cu layer is relatively thick, there is no appreciable coupling between the two FM layers, and so the top (free) FM can be rotated by a small magnetic field. Field sensing by the GMR effect is accomplished by the relative orientations of the two FM layers.

In 1993, a large MR effect in manganites (e.g., La–Ca–Mn–O) was rediscovered and christened the colossal MR (CMR) effect, because the effect can indeed be very large (e.g., 10^5%).[8,9] The large MR effect in the CMR materials is realized in the vicinity of a metal-insulator transition. Because both the CMR and the GMR effects are magnetic in origin, they exhibit negative MR in all measuring geometries with magnetic hysteresis and a complex field dependence, unsuitable for wide-range field sensing.

The simplest of all MR effects is the ordinary MR (OMR), which exists in all metals and alloys due to curving of the charge carriers' trajectories in a magnetic field. OMR has a quadratic field dependence and is usually quite small in common metals such as Cu and Au. However, with a favorable combination of electronic properties, as realized in semimetallic bismuth (Bi), the OMR effect can in fact be very large, much larger even than the largest GMR effect ever reported.[10,11] The most important quantity for OMR is $\omega_c\tau$, where $\omega_c = eH/m^*c$ is the cyclotron frequency, τ is the carrier scattering time, and m^* is the effective carrier mass. The carrier scattering time τ is related to the carrier mean free path $l = \nu_F\tau$ and the conductivity $\sigma = ne^2\tau/m^*$, where ν_F is the Fermi velocity and n is the carrier concentration. It is straightforward to show that $\omega_c\tau = H\sigma/nec$. Physically, $\omega_c\tau$ is the turn angle in radians within the scattering time τ during the spiraling motion of the carriers in a magnetic field. To have a substantial MR, $\omega_c\tau$ should be at least of order 1. It is useful to compare the differences between the electronic properties of Cu and Bi. Because of its semimetallic nature, there are both holes and electrons in Bi, and the mobility of the electrons is much larger than that of the holes. With a low carrier concentration of $n = 3\times10^{23}/\mathrm{m}^3$, the values of n and the Hall constant $R_H = 1/nec$ for Bi are, respectively, five orders of magnitude smaller and larger than those of Cu.[12] The effective carrier mass m^* and the con-

[a]Electronic mail: CLC@pha.jhu.edu

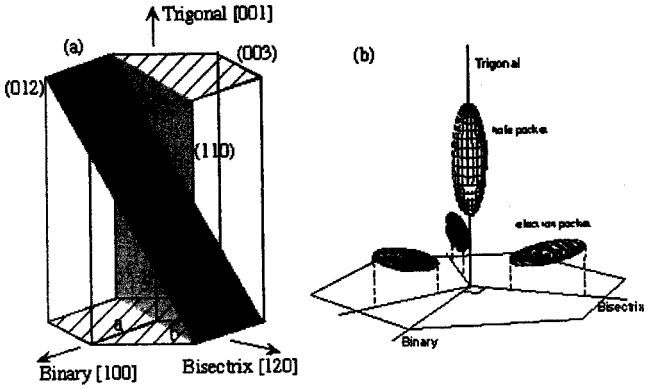

FIG. 1. (a) Crystal structure of Bi indexed in a hexagonal system showing the (003), (012), and the (110) planes and the trigonal [001], binary [100] and the bisectrix [120] axes, and (b) schematic of the Fermi surface of Bi showing the hole pocket along the trigonal axis and three electron pockets above the bisectrix axes.

ductivity σ of Bi are about two orders of magnitude smaller than that of Cu at room temperature. Simple calculations using the nearly free electron model (which is a reasonable one for Cu but a poor approximation for Bi) show that $\omega_c\tau$ for Cu is $5\times10^{-3}H$ for Cu and $1.5H$ for Bi, and thus, for a given field value H, one expects that the MR effect in Bi will be much larger than that in Cu. Indeed, for laboratory magnetic fields on the order of a few T, the MR is negligible in Cu($\omega_c\tau\ll1$) but very large in Bi($\omega_c\tau\gg1$).

The earlier simple analyses show that very large MR effects can be observed in Bi samples *with* a very long mean free path l. This has been realized in bulk Bi single crystals with l in excess of 100 μm that show MR as much as 10^6 times at low temperatures.[11] Due to its unusual electronic properties (e.g., very long Fermi wavelength of 400 Å)[13] and a long l, Bi is also a unique medium for exploring quantum and ballistic transport properties.[14–16] For such studies as well as for capturing the large MR effect for technological purposes, Bi in thin film form is required. Unfortunately, high quality Bi thin films are notoriously difficult to produce. Thin films of Bi fabricated by traditional deposition techniques (evaporation, sputtering, and pulsed laser ablation) are usually polycrystalline with small grains (e.g., 10 nm).[17,18] These small grains are common for polycrystalline metal films but unacceptable for achieving a large MR in Bi, because the small grains result in a small l, and hence, a miniscule MR effect. Recently, high quality Bi thin films have been produced by molecular beam epitaxy on BaF_2 substrates, a well controlled but slow and costly venture.[16,19] In the last year, we have reported a new method using electrodeposition to fabricate high quality Bi thin films, which exhibit an enormous MR effect.[20,21]

Bi has a low melting point of 271.4 °C and a rhombohedral structure, which is slightly distorted from a cubic structure. Its structure is often described as a hexagonal system as shown in Fig. 1(a), in which the (001), the (110), and the (012) planes, which are of significance as described later, are also shown. The Fermi surface, consisting of both hole and electron pockets, is highly anisotropic. The cigar-shaped hole pocket is along the [001] axis, or the trigonal axis. There are three equivalent cigar-shaped electron pockets located symmetrically about the trigonal axis that lie essentially in the c plane, with a slight tilt of about 6°. The centers of the electron pockets are situated directly above the bisectrix axis. The binary axis is perpendicular to the trigonal and bisectrix axes. The magnetotransport properties of Bi are therefore highly anisotropic, depending sensitively on the orientation of the external magnetic field with respect to the crystal axes.

Recently, during the course of our exploration of the fabrication of Bi nanowire arrays into nanoporous templates,[22,23] in which electrodeposition is the only viable method, we have found electrodeposition to be a superior deposition method for fabricating high quality Bi thin films.[20,21] After further processing, these electrodeposited films become single-crystals Bi thin films, in which we have observed enormous MR effects of as much as 400 000% at low temperatures and 300% at room temperature, and pronounced Shubnikov–de Haas (S–dH) oscillations.[24] To illustrate the potential of Bi films for sensing magnetic fields, we have used a simple hybrid structure, with which a large MR effect of 30% at 200 Oe with a field sensitivity of 0.2%/Oe at room temperature has been achieved. These results show that the electrodeposited Bi thin films are new media for the study of the unusual transport properties of Bi and for the development of field-sensing devices.

FABRICATION AND STRUCTURAL CHARACTERIZATION

Bi thin films were fabricated by electrodeposition from aqueous solution of $Bi(NO_3)_3\cdot5H_2O$ onto thin Au underlayers (about 100 Å thick) patterned onto Si substrates as reported elsewhere.[22,21] The as-deposited Bi films, 1–20 μm thick, are polycrystalline but with very large grains, whose sizes are comparable to the film thickness. This fact alone is a marked improvement over traditional thin film fabrication methods. Additional advantages of electrodeposition are the high deposition rate of about 0.2 μm/min, which is one to two orders of magnitude higher than those of other deposition methods, and the ability to coat surfaces of irregular shapes. Upon annealing the Bi films in Ar, the polycrystalline samples go through rapid grain growth and eventually transform into single crystals near 268 °C.[20,21]

In most, but not all cases, the final Bi thin films are trigonal-axis [001] oriented. As an example, Fig. 2 shows the $\theta/2\theta$ x-ray patterns of representative samples cut from one electrodeposited specimen, 5 μm thick, after annealing at various temperatures T_A. The as-prepared film [Fig. 2(a)] is polycrystalline with large grains. Upon annealing at $T_A>150\,^\circ$C, there are noticeable changes in the intensities in the x-ray pattern due to grain growth. The most important development is the rapid growth of the (003) peak. At $T_A=268\,^\circ$C, as shown in Fig. 2(d) only the (003), (006), and (009) peaks are observed, i.e., the sample is a trigonal-axis [001] oriented film. X-ray pole-figure measurements (with a sampling area of about 4 mm^2) were used to measure the off-axis peaks in order to determine the in-plane coherence. Pole-figure measurements of the off-axis (012)[shown in Fig. 3(c)], (116), and (202) peaks, taken at tilt angles 57.5°, 41°, and 69° respectively, show the expected threefold, sixfold,

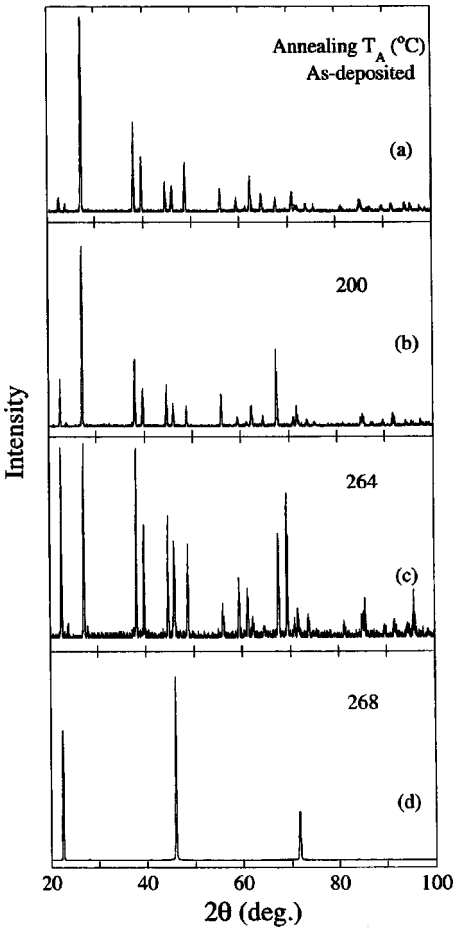

FIG. 2. $\theta/2\theta$ x-ray diffraction patterns of (a) as-prepared 5-μm-thick Bi film and those annealed at temperatures T_A of (b) 200, (c) 264, and (d) 268 °C.

and threefold symmetries, and more importantly, with the *same* orientations at various locations of the film. These results demonstrate that the electrodeposited Bi film after annealing at 268 °C has unique in-plane and out-of-plane crystal orientations, as that of a single-crystal film. We have investigated the roles of the Au underlayer and Si substrates and concluded that they are unlikely sources for epitaxy.

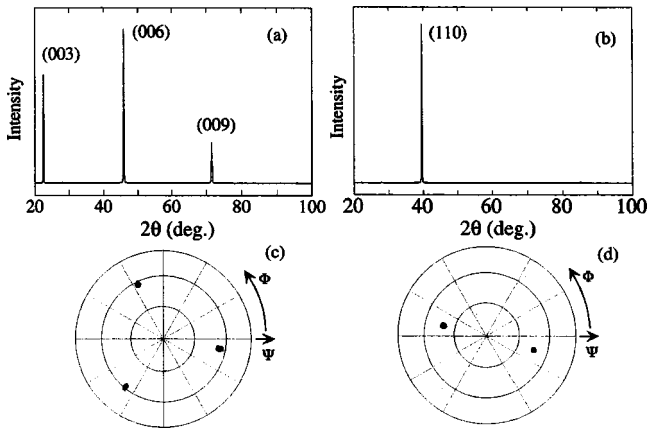

FIG. 3. $\theta/2\theta$ x-ray diffraction patterns of (a) the [001] and (b) the [110] oriented Bi films, and the pole-figure measurements of (c) the [001] film at tilt angle 57.5° and (d) the [110] film at tilt angle 42°.

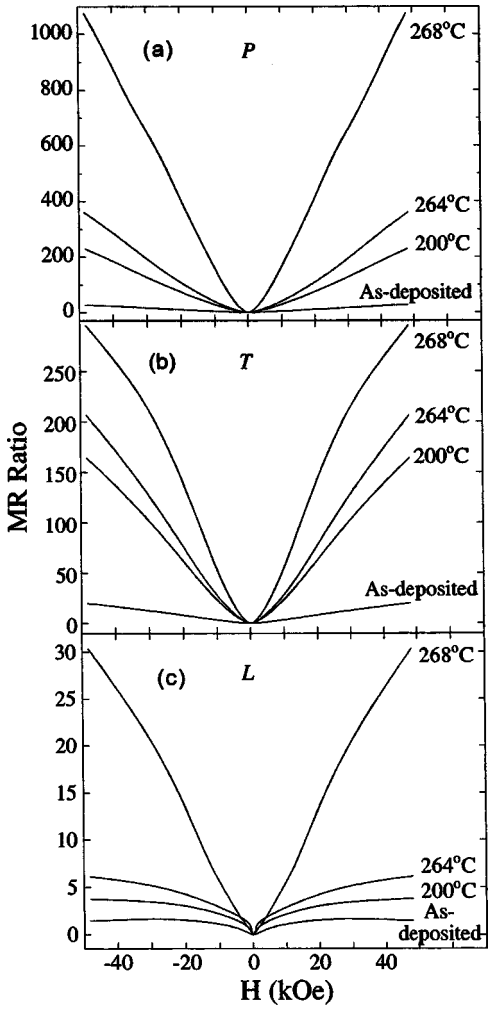

FIG. 4. MR results in the (a) perpendicular (*P*), (b) transverse (*T*), and (c) longitudinal (*L*) geometry of 5-μm-thick Bi films annealed at different temperatures.

While many trigonal-axis [001] oriented films have been made, we have also obtained [110] [Fig. 3(b)] and [012] oriented (not shown) Bi films by varying the deposition conditions. The pole-figure measurement of (012) peak shown in Fig. 3(d) illustrates that the [110] film is also a single crystal. The relevant (001), (110), and the (012) planes are shown in Fig. 1(a). It appears that the final crystal orientation depends on the details of the electrodeposition conditions, and further investigations are underway. We have observed at least three different orientations of [001], [110], and the [014]. In the following only the MR results of the trigonal [001] films are described.

MR

The growth and the reorientation of the [001] grains upon annealing dramatically increase the magnitude of the MR effect as shown Fig. 4 for a series of 5-μm-thick Bi films, cut from one as-deposited specimen. Here the MR effect is described as the MR ratio $[\rho(H)/\rho(0)]$, where ρ is the resistivity. Later on, the MR effect will also be displayed in percent $\{[\rho(H)-\rho(0)]/\rho(0)\times 100\%\}$. For example, a MR ratio of 300 is approximately a MR effect of 30 000%.

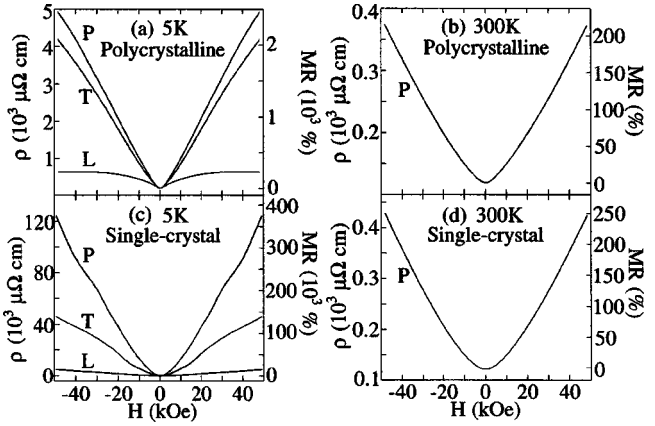

FIG. 5. MR results of a 20-μm-thick polycrystalline Bi film at (a) 5 and (b) 300 K, and a 20-μm-thick single-crystal Bi film at (c) 5 and (d) 300 K in the perpendicular (P), transverse (T), and longitudinal (L) geometry.

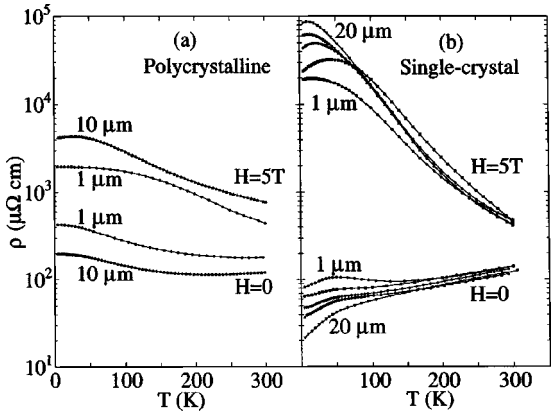

FIG. 6. Temperature dependence of resistivity ρ at $H=0$ and at 5 T of (a) polycrystalline Bi films 1 and 10 μm thick, and (b) single-crystal films 1–20 μm thick. In (b), the curves at low temperature are in decreasing [$\rho(0)$] and increasing [$\rho(5\ \mathrm{T})$] order for thickness 1, 2, 5, 10, and 20 μm.

The MR has been measured in the perpendicular (P), transverse (T), and longitudinal (L) geometries, where the magnetic field **H** is applied perpendicular to the film plane in the P geometry, in-plane and perpendicular to current in the T geometry, and in-plane and parallel to current in the L geometry. It is clear in Fig. 4 that annealing at higher T_A dramatically increases the MR effect in all geometries, until $T_A = 268\,^{\circ}\mathrm{C}$, above which little difference has been observed.

The MR characteristics in the P, T, and L geometries for the 20 μm polycrystalline and single-crystal films at 5 and 300 K are shown in Fig. 5. In the case of the single-crystal trigonal [001] films, we have used x-ray diffraction to determine the crystal axes of the film so that in the P, T, and L geometries, the magnetic field has been applied along the trigonal, the binary, and the bisectrix axes of Bi, respectively. First of all, one notes the very large MR in the single-crystal film, with a MR ratio of nearly 4000, or 400 000%, in the P geometry. At 300 K, the magnitude is drastically reduced to only about 250%.

In both the polycrystalline and the single-crystal films, the transverse MR is always larger than the longitudinal MR. This is simply due to the orientation of the cyclotron orbits with respect to the film geometry. In the L geometry, MR would be zero if the motion of all the carriers is exactly parallel to **H**. Within the T and the L geometry, we have found the angular dependence of MR of $(1-\cos\theta)$ for **H** in the film plane, where θ is the angle between **H** and the current. In Bi thin films, there is also a significant difference between the perpendicular MR and the transverse MR as shown in Fig. 5, where the perpendicular MR is the largest of all. This difference, due to the thickness of the films, becomes negligible for very thick films.

TEMPERATURE AND THICKNESS DEPENDENCE OF RESISTIVITY

The temperature dependence of the resistivity at zero field $\rho(0)$ and at 5 T $\rho(5\ \mathrm{T})$ of the polycrystalline and the single-crystal Bi films of 1–20 μm thick are shown in Fig. 6. In the case of the polycrystalline films, both $\rho(0)$ and $\rho(5\ \mathrm{T})$, and hence, the MR ratio $\rho(5\ \mathrm{T})/\rho(0)$, have a relatively weak temperature dependence. In the single-crystal films at low temperatures, $\rho(0)$ is much lower and $\rho(5\ \mathrm{T})$ is much higher, hence, the MR ratio $\rho(5\ \mathrm{T})/\rho(0)$ is much larger than those of the polycrystalline counterparts. All of these quantities for the single-crystal films have a relatively stronger temperature dependence due to that of the carrier mean free path. However, at room temperature, the values of $\rho(0)$, $\rho(5\ \mathrm{T})$, and hence, $\rho(5\ \mathrm{T})/\rho(0)$, for the polycrystalline and the single-crystal Bi thin films are similar in values. Thus, as far as the MR effect at room temperature is concerned, as would be relevant for technological applications, the as-prepared polycrystalline samples with large grains would suffice.

The effective carrier mean free path l_{eff} of the single-crystal films has been determined for Bi thin films 1–20 μm thick.[21] In each case, l_{eff} is comparable to, and usually slightly less than, the film thickness. This indicates that intrinsic carrier mean free path l in the Bi films is longer than this, and the measured l_{eff} is limited by the film thickness. It should be noted that carrier mean free paths of the order of 10 nm are common in most metal films. It is rare that carrier mean free paths of tens of microns, as obtained in the Bi films, are realized. This suggests that one can exploit the enormous carrier mean free path in Bi and use Bi thin films as electrical interconnects between other entities, through which the characteristics of the carriers can be preserved.

Also due to the thickness-limited l_{eff} both $\rho(0)$ and $\rho(5\ \mathrm{T})$, and therefore the MR ratio of $[\rho(5\ \mathrm{T})-\rho(0)]/\rho(0)$ depend on the film thickness t. Using the results from the single-crystal [001] films at 5 K in the thickness range of 1–20 μm, we find that $\rho(0)\approx 82\times t^{-0.43}\,\mu\Omega\,\mathrm{cm}$, $\rho(5\ \mathrm{T})\approx 20000\times t^{0.5}\,\mu\Omega\,\mathrm{cm}$, and MR ratio $=\rho(5\ \mathrm{T})/\rho(0)\approx 240\times t^{0.93}$, where t is in microns. Extrapolating from such a dependence, a film of 400 Å thick would still give a MR effect of 1200%, and a 55-μm-thick film would give a MR ratio of 10^4, or a 10^6% MR effect at low temperatures.

S–dH OSCILLATIONS

In Fig. 5, one notes the field dependence of the MR of the single-crystal Bi films is not smooth but contains oscil-

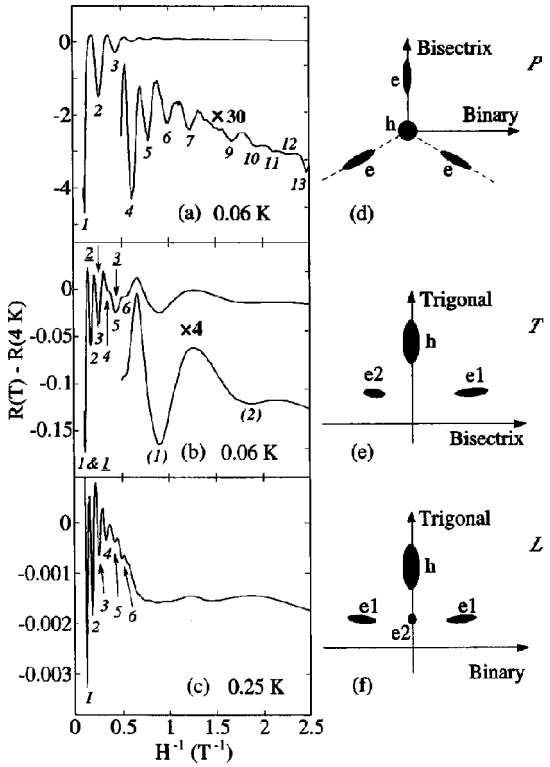

FIG. 7. S–dH oscillation vs $1/H$ in (a) perpendicular and (b) transverse geometry at 0.06 K, and (c) longitudinal geometry at 0.25 K with order n indicated. In (b) the numbers with underlines and parenthesis are from electron bands $e1$ and $e2$, and the numbers from 1 to 6 are from the hole band h. The extremal cross sections of the Fermi surface perpendicular to H are shown in (d) perpendicular, (e) transverse, and (f) longitudinal geometries.

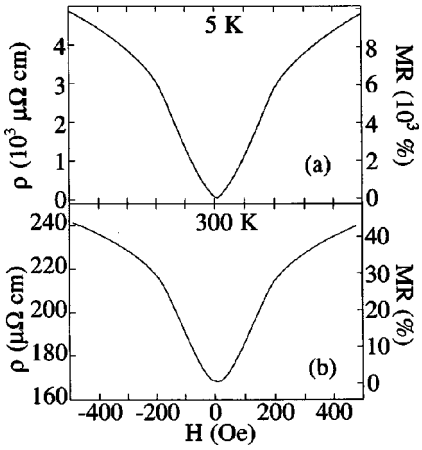

FIG. 8. MR of an as-prepared Bi film placed at the end of a small Fe slab at (a) 5 and (b) 300 K.

lations. These are the S–dH oscillations, historically first discovered in bulk Bi single crystals.[25] The S–dH oscillations are due to the Landau quantization of the cyclotron orbits of the carriers.[26] With increasing magnetic field, the occupancy of each Landau level and the separation between adjacent Landau levels ($\hbar\omega_c$) become larger. As a result, the Landau levels below the Fermi level are sequentially driven across the Fermi level, with an accompanying changes in the density of states. The S–dH oscillations are periodic in $1/H$ with a period of $\Delta(1/H)=2\pi e/\hbar Ac$, inversely proportional to the extremal cross-sectional area A of the Fermi surface in the plane normal to **H**. Because the Fermi surfaces of Bi for both holes and electrons are highly anisotropic, as shown in Fig. 1(b) the S–dH oscillations display distinct periods when **H** is applied along various crystal axes. Thus, the measurement of the S–dH oscillations is another stringent test of the quality of the Bi films.

The results of the S–dH oscillations in the *P*, *T*, *L* geometries with **H** along the trigonal, the bisectrix and the binary axes, measured at 0.06, 0.06, and 0.25 K respectively, are shown in Fig. 7 as a function of $1/H$. These measurement were made at low temperatures, because the amplitude of the S–dH oscillations increases with decreasing temperature until the Dingle temperature $T_D=\hbar/k_B\tau$.[26] It turns out that for the Bi films, T_D is about 0.4 K. Hence, at 0.25 K and below, there is no appreciable temperature dependence in the S–dH oscillations. To display more clearly the S–dH results, we have subtracted the MR values at 4 K, which contain little S–dH oscillations, from the measured MR at low temperatures. Also shown in Fig. 7 are the extremal cross sections of the Fermi surfaces in the three geometries studied. Electron bands with different extremal cross-sectional areas have been labeled with $e1$ and $e2$. In the *P* geometry, the cross-sectional areas of the hole and the electron pockets turn out to be nearly the same. Thus, the S–dH oscillations with effectively a single period up to 13th order have been observed. In the *T* geometry, three oscillation periods corresponding to one hole pocket and two electron pockets have been observed. In the *L* geometry, in part because of the much smaller MR, only the period of the hole pocket can be clearly observed up to sixth order. The observed periods in all three geometries are in good agreement with those obtained in bulk Bi single crystals.[27] The S–dH oscillation results further attest to the high quality of the single-crystal Bi films.

POTENTIAL APPLICATIONS

As shown in Fig. 5, the very large MR effect in Bi thin films is nonhysteretic because Bi is nonmagnetic. It has a quasilinear field dependence similar to the Hall effect, and the MR does not saturate, which is also different from both GMR and CMR. These characteristics are favorable for applications in wide-range field and current sensing. With suitable hybrid structures, the MR effect in Bi films may also be used to detect small magnetic fields. By taking advantage of the strong response to small magnetic fields of soft magnetic materials, a large MR can be realized in a Bi element placed in the vicinity of ferromagnetic materials. As an example, the MR effect at 5 and 300 K, measured from a simple hybrid structure of a Bi film placed at the end face of a small Fe slab, is shown in Fig. 8. A large MR effect of 6000% at 200 Oe with a field sensitivity of 35%/Oe at 5 K and 30% MR at 200 Oe with a sensitivity of 0.2%/Oe at 300 K have been realized. The very high sensitivity of 35%/Oe, with a large dynamic range at low temperatures, can potentially be used to detect magnetic fields generated by small structures such as magnetic dots and superconducting rings. The sensitivity of 0.2%/Oe at 300 K is similar to that of the AMR effect in

permalloy. With a better design of the hybrid structures and field concentrators, a much larger MR effect with higher sensitivities can be expected.

SUMMARY

Using electrodeposition we have fabricated high quality Bi thin films. With further processing, the Bi films become single crystal with long carrier mean free paths. The high quality of the Bi films is further endorsed by the observation of very large MR effects and pronounced S–dH oscillations. The as-deposited Bi thin films can also be used as wide-range field and current sensors and for sensing small magnetic fields in hybrid structures. Finally, these Bi thin films with very long carrier mean free path provide a favorable medium for exploring quantum and ballistic transport unique to Bi films as well as for phase-preserving interconnects.

ACKNOWLEDGMENTS

Work supported by NSF Grant Nos. DMR96-32526, DMR97-32763, and DMR93-57518.

[1] See, e.g., T. R. McGuire and R. I. Potter, IEEE Trans. Magn. **MAG–11**, 1018 (1975).
[2] M. N. Baibich *et al.*, Phys. Rev. Lett. **61**, 2472 (1988).
[3] S. S. P. Parkin, R. Bhadra, and K. P. Roche, Phys. Rev. Lett. **66**, 2152 (1991).
[4] A. E. Berkowitz *et al.*, Phys. Rev. Lett. **68**, 3745 (1992).
[5] J. Q. Xiao, J. S. Jiang, and C. L. Chien, Phys. Rev. Lett. **68**, 3749 (1992).
[6] E. E. Fullerton, M. J. Conover, J. E. Mattson, C. H. Sowers, and S. D. Bader, Appl. Phys. Lett. **63**, 1699 (1993); Phys. Rev. B **48**, 15755 (1993).
[7] B. Dieny, V. S. Speriosu, S. S. P. Parkin, B. A. Gurney, D. R. Wilhoit, and D. Mauri, Phys. Rev. B **43**, 1297 (1991).
[8] R. von Helmolt, J. Wecker, B. Holzapfel, L. Schultz, and K. Samwer, Phys. Rev. Lett. **71**, 2331 (1993).
[9] S. Jin, T. H. Tiefel, M. MaCormack, R. A. Fastnact, R. Ramesh, and L. H. Chen, Science **264**, 413 (1994).
[10] J. H. Mangez, J.-P. Issi, and J. Heremans, Phys. Rev. B **14**, 4381 (1976).
[11] P. B. Alers and R. T. Webber, Phys. Rev. **91**, 1060 (1953).
[12] D. H. Reneker, Phys. Rev. Lett. **1**, 440 (1958); W. S. Boyle and G. E. Smith, Prog. Semicond. **7**, 1 (1963).
[13] N. Garcia, Y. H. Kao, and M. Strongin, Phys. Rev. B **5**, 2029 (1972).
[14] Y. F. Komnik, E. I. Bukhshtab, Y. V. Nikitin, and V. V. Andrievskii, Zh. Eksp. Teor. Fiz. **60**, 669 (1971) [Sov. Phys. JETP **33**, 364 (1971)].
[15] C. A. Hoffmann *et al.*, Phys. Rev. B **48**, 11431 (1993).
[16] M. Lu, R. J. Zieve, A. van Hulst, H. M. Jaeger, T. F. Rosenbaum, and S. Radelaar, Phys. Rev. B **53**, 1609 (1996).
[17] D. E. Beutler and N. Giordano, Phys. Rev. B **38**, 8 (1988).
[18] T. Missana and C. N. Afonso, Appl. Phys. A: Mater. Sci. Process. **62**, 513 (1996).
[19] D. L. Partin, J. Heremans, D. T. Morelli, C. M. Thrush, C. H. Olk, and T. A. Perry, Phys. Rev. B **38**, 3818 (1988).
[20] F. Y. Yang, K. Liu, C. L. Chien, and P. C. Searson, Phys. Rev. Lett. **82**, 3328 (1999).
[21] F. Y. Yang, K. Liu, K. Hong, D. H. Reich, P. C. Searson, and C. L. Chien, Science **284**, 1335 (1999).
[22] K. Liu, C. L. Chien, P. C. Searson, and K. Yu-Zhang, Appl. Phys. Lett. **73**, 1436 (1998).
[23] K. Liu, C. L. Chien, and P. C. Searson, Phys. Rev. B **58**, R14681 (1998).
[24] F. Y. Yang *et al.*, Phys. Rev. B (submitted).
[25] L. W. Shubnikow and W. J. de Haas, Proc. Acad. Sci. Amsterdam **33**, 130 (1930); **33**, 363 (1930); **33**, 418 (1930).
[26] J. M. Ziman, *Principles of the Theory of Solids* (Cambridge University Press, Cambridge, 1964).
[27] G. E. Smith, G. A. Baraff, and J. M. Rowell, Phys. Rev. **135**, A1118 (1964).